

Laboratory and Astronomical Discovery of HydroMagnesium Isocyanide ¹

C. Cabezas

*Grupo de Espectroscopia Molecular (GEM), Unidad Asociada CSIC, Edificio Quifima.
Laboratorios de Espectroscopia y Bioespectroscopia. Universidad de Valladolid, 47005
Valladolid, Spain*

ccabezas@qf.uva.es

J. Cernicharo

*Department of Astrophysics, CAB. INTA-CSIC. Crta Torrejón-Ajalvir Km 4. 28850
Torrejón de Ardoz, Madrid, Spain*

and

J.L. Alonso

*Grupo de Espectroscopia Molecular (GEM), Unidad Asociada CSIC, Edificio Quifima.
Laboratorios de Espectroscopia y Bioespectroscopia. Universidad de Valladolid, 47005
Valladolid, Spain*

and

M. Agúndez

University of Bordeaux, LAB, UMR 5804, F-33270 Floirac, France

and

S. Mata

*Grupo de Espectroscopia Molecular (GEM), Unidad Asociada CSIC, Edificio Quifima.
Laboratorios de Espectroscopia y Bioespectroscopia. Universidad de Valladolid, 47005
Valladolid, Spain*

and

M. Guélin

*Institut de Radioastronomie Millimétrique, 300 rue de la Piscine, 38406 Saint Martin
dHères, France*

and

I. Peña

*Grupo de Espectroscopia Molecular (GEM), Unidad Asociada CSIC, Edificio Quifima.
Laboratorios de Espectroscopia y Bioespectroscopia. Universidad de Valladolid, 47005
Valladolid, Spain*

ABSTRACT

We report on the detection of hydromagnesium isocyanide, HMgNC, in the laboratory and in the carbon rich evolved star IRC+10216. The J=1-0 and J=2-1 lines were observed in our microwave laboratory equipment in Valladolid with a spectral accuracy of 3 KHz. The hyperfine structure produced by the Nitrogen atom was resolved for both transitions. The derived rotational constants from the laboratory data are $B_0=5481.4333(6)$ MHz, $D_0=2.90(8)$ KHz, and $eQq(N)=-2.200(2)$ MHz.

The predicted frequencies for the rotational transitions of HMgNC in the millimeter domain have an accuracy of 0.2-0.7 MHz. Four rotational lines of this species, J=8-7, J=10-9, J=12-11 and J=13-12, have been detected towards IRC+10216. The differences between observed and calculated frequencies are <0.5 MHz. The rotational constants derived from space frequencies are $B_0=5481.49(3)$ MHz and $D_0=3.2(1)$ KHz, i.e., identical to the laboratory ones. A merged fit to the laboratory and space frequencies provides $B_0=5481.4336(4)$ MHz and $D_0=2.94(5)$ KHz.

We have derived a column density for HMgNC of $(6\pm 2)\times 10^{11}$ cm⁻². From the observed line profiles the molecule have to be produced produced in the layer where other metal-isocyanides have been already found in this source. The abundance ratio between MgNC and its hydrogenated variety, HMgNC, is $\simeq 20$.

Subject headings: ISM: abundances — ISM: individual objects (IRC+10216) — ISM: molecules — line: identification — molecular data

To appear in the Astrophysical Journal September 2013

¹This work was based on observations carried out with the IRAM 30-meter telescope. IRAM is supported by INSU/CNRS (France), MPG (Germany) and IGN (Spain)

1. Introduction

Metal-bearing molecules, NaCl, KCl, AlF, and NaF, were detected 30 years ago in the circumstellar envelope (CSE) of the carbon-rich star envelope IRC+10216 by Cernicharo & Guélin (1987). This species were predicted to be produced under thermodynamical chemical equilibrium near the photosphere of the star (Tsuji 1973). Just a few months before these detections Guélin et al. (1986) reported on the presence of a new free radical in IRC+10216. Several Silicon and Sulfur bearing candidates were proposed at that time, but the line carrier was definitively identified as MgNC only years latter from laboratory measurements Kawaguchi et al. (1993). The emission of magnesium isocyanide was mapped in IRC+10216 with the IRAM Plateau de Bure Interferometer by Guélin, Lucas and Cernicharo (1993). Unlike metal-halogen species that are formed near the star photosphere, MgNC was found in a thin shell 15" in radius where many reactive species such as the carbon chain radicals C₅H, C₆H, C₇H, and C₈H, are also detected (Cernicharo et al. 1986a,b; Guélin et al. 1987; Cernicharo et al. 1987a,b; Cernicharo & Guélin 1996; Guélin et al. 1997). Just one year after the identification of MgNC, sodium cyanide was also detected in IRC+10216 by Turner et al. (1994). MgNC has been also found towards the more evolved carbon star CRL2688 (Highberger et al. 2003).

It is worth noting that metals such as Na, K, Ca, Fe, Cr, and/or their cations are found in the gas phase in IRC+10216 (Mauron & Huggins 2010) pointing towards a rich metal chemistry in the outer circumstellar envelope (CSE). Since these early works several more metal cyanides or isocyanides have been found in CSEs. MgCN, AlNC, SiCN, SiNC, KCN, and FeCN have been identified in IRC+10216 after their mm-wave rotational spectrum has been characterized in the spectroscopic laboratory (Ziurys et al. 1995, 2002; Guélin et al. 2000, 2004; Pulliam et al. 2010; Zack et al. 2011). Many other have been searched for in the same way without success. We note that TiO and TiO₂ have recently been detected in the Oxygen-rich CSE V_yCMa (Kaminski et al. 2013).

While some metal-bearing species containing Al, Na or K are stable closed shell molecules that mostly form in the hot part of the envelope, close to the star, other, containing Mg, Si or Fe, are open shell radicals that react even at low temperature with neutral molecules or atoms and may be formed in the outer envelope. MgNC and MgCN remain the only Mg-bearing species detected in space so far. The chemistry of these molecules could be based on the reaction of Mg⁺ with other molecules formed in the CSE (Petrie 1996; Dunbar & Petrie 2002). The detection of additional Mg-bearing species could allow a detailed chemical analysis of the reactions leading to the formation of these molecules and to help in discriminating between gas phase chemical paths or dust grain surface reactions. The adjunction of an hydrogen atom to the radicals MgNC and SiCN yields stable closed shell molecules that may

be thought to be more abundant. Despite the characterization of their mm spectra in the laboratory (Sanz et al. 2002), HSiCN and HSiNC have not been detected so far in space.

The most abundant metal cyanide being MgNC, it was interesting to see if HMgNC is present. In this Letter we report on the detection in the laboratory and in space of Hydrogenated Magnesium Isocyanide, HMgNC and we perform detailed chemical models to analyse the formation mechanisms of these metal-bearing species.

2. Laboratory Characterization of HMgNC

The HMgNC spectrum was measured using a laser ablation molecular beam Fourier transform microwave (LA-MB-FTMW) spectrometer at the University of Valladolid, which operates in the 4-26 GHz frequency range and is described elsewhere (Alonso et al. 2009). HMgNC was created by laser ablation of magnesium rods in the throat of a pulsed supersonic expansion of highly diluted ethylcyanide (0.2%) in Neon (15 bars stagnation pressure) using a pulsed Nd:YAG-laser ($\lambda = 355$ nm, $\simeq 20$ mJ pulse⁻¹) focused on the rod for ablation at a repetition rate of 2 Hz. The rod was continuously rotated and translated in order to minimizing the problem of shot-to-shot fluctuation in the amount of the desorbed material. Briefly, the sequence of an experimental cycle starts with a gas pulse of the mixing carrier gas (typically 450 μ s). After an adequate delay, a laser pulse hits the metal rod producing the vaporization of the solid and the chemical reaction in the precursors mixture (Cabezas et al. 2012). Immediately, the resulting products are supersonically expanded between the two mirrors of the Fabry-Pèrot resonator and then a microwave pulse ($\simeq 0.3$ μ s) is applied, producing the macroscopic polarization of the species in the jet. Once the excitation ceases, molecular relaxation gives rise to a transient emission signal (free induction decay) at microwave frequencies, which is captured in the time domain. Its Fourier transformation to the frequency domain yields the rotational transitions that appear as Doppler doublets, because the supersonic jet travels parallel to the resonator axis (see Figure 1). The molecular rest frequencies are calculated as the arithmetic mean of the Doppler doublets, and are obtained with accuracy better than 3 kHz.

To optimize the experimental conditions for HMgNC, we tested the J= 1-0 transition for the radical MgNC (Kawaguchi et al. 1993; Walker & Gerry 1998) due to the similarities between both molecules. A previous theoretical work available in the literature predicts the rotational constant for HMgNC molecule around $B_0 \simeq 5438.2$ MHz (Gronowski & Kolos 2013). We have carried out ab initio calculations at MP2/6-311++G(d,p) level of theory to predict another parameter relevant to our experiment, the nitrogen (I=1) quadrupole coupling constant for which we obtain $eQq = -1.95$ MHz. Frequency scans were conducted to

search for the J= 1-0 transition around the 11 GHz range. We finally found a set, composed of three lines (Figure 1) in the region of 10962 MHz for which frequency separation was very similar to the expected one, taking into consideration the nitrogen eQq value. No other fine or hyperfine structure arising from spin-rotation interactions was observed, indicating that the observed spectrum arises from a closed-shell molecule. The next J transition was then observed, leading to the unambiguous assignment of HMgNC as a linear molecule, since five new hyperfine components were measured in the 21.9 GHz region. Table 1 lists J= 1-0 and J= 2-1 rotational transitions for HMgNC labeled by quantum number F, where $F=J+I$. To analyze them we have used a Hamiltonian of the following form: $H = H_R + H_Q$ where H_R contains rotational and centrifugal distortion parameters while H_Q the quadrupole coupling interactions. We obtain $B_0=5481.4333(6)$ MHz, $D_0=2.90(8)$ KHz, and $eQq(N)=-2.200(2)$ MHz. The standard deviation of the fit is 1.6 KHz.

3. Astronomical Observations and identification of HMgNC

The observations were performed at the IRAM 30m telescope at Pico Veleta (Spain). Many different runs have been used for the present observations covering the period 1990-2010. Hence, different receivers and spectrometers have been used. The spectral resolution has been always 1 MHz. Receiver temperatures were around 150 K in the early observations and have been improving with time down to 50-60 K in the last observing runs. All the observations were performed using the Wobbler Switching mode which produces remarkable flat baselines. Pointing errors were always within 3". The 30m beam size at the observing frequencies ranges from 29" for the J=8-7 transition to the 17" of the J=13-12 line. The spectra were calibrated in antenna temperature corrected for atmospheric attenuation using the ATM package (Cernicharo 1985; Pardo et al. 2001). Most of the 3 mm data pertain to a line survey that will be published elsewhere (Cernicharo et al., 2013, in preparation).

The rotational constants of HMgNC determined in the laboratory have been implemented in MADEX (Cernicharo 2012). We have adopted the dipole moment, 3.49 D, predicted from the *ab initio* calculations of Gronowski & Kolos (2013). Four features in harmonic relation 8:10:12:13 have been found in IRC+10216 and are assigned to the rotational transitions J=8-7, 10-9, 12-11, and 13-12 of HMgNC. The lines are shown in Figure 2 and their frequencies are given in Table 1. Using our MADEX catalogue we conclude that none of these lines agrees in frequency with any isotopologue or vibrational level of already known molecular species. From a fit to the observed frequencies we obtain $B_0=5481.49(3)$ MHz and $D_0=3.2(1)$ KHz, i.e., near identical to the rotational constants obtained in the laboratory. The J=8-7 and J=10-9 transitions are unblended with other features and are clearly

Table 1. Laboratory and Space Frequencies for the observed transitions of HMgNC

J_u	F_u	J_l	F_l	$\nu(\text{MHz})$	Unc(MHz)	$\nu_o-\nu_c(\text{KHz})$
1	1	0	1	10962.305	0.002	0.2
1	2	0	1	10962.966	0.002	0.3
1	0	0	1	10963.954	0.002	-1.8
2	2	1	2	21924.979	0.002	-1.2
2	1	1	0	21925.089	0.002	-1.5
2	2	1	1	21925.643	0.002	2.5
2	3	1	2	21925.688	0.002	0.5
2	1	1	1	21926.741	0.002	0.4
3		2		32888.284	0.003	predicted
4		3		43850.716	0.009	predicted
5		4		54812.866	0.019	predicted
6		5		65774.663	0.035	predicted
7		6		76736.036	0.058	predicted
8		7		87697.500	0.400	584.5
10		9		109616.700	0.400	-210.4
12		11		131533.900	1.000	-182.6
13		12		142490.900	1.000	-533.8
14		13		153447.868	0.489	predicted
15		14		164403.313	0.603	predicted
16		15		175357.701	0.733	predicted
17		16		186310.959	0.881	predicted
18		17		197263.018	1.048	predicted
19		18		208213.806	1.233	predicted

Note. — The J=1-0 and J=2-1 lines have been observed in the laboratory with an accuracy of 2 KHz. The lines J=8-7, 10-9, 12-11 and 13-12 have been observed in IRC+10216. Predictions obtained with the derived rotational constants are provided for lines with $E_{upp} < 100$ K.

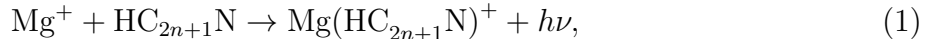
detected. The J=9-8 line is predicted at 98657.3(2) MHz and is fully blended with the the $11_{1,10}$ - $10_{1,9}$ line of H_2C_4 at 98655.094(4) MHz. Hence, it is not show in Figure 2. The J=11-10 line at 120576 MHz is fully blocked by the Earth atmosphere. The J=10-9 line of HMgNC at 109616.3 MHz agrees with the J=12-11 $l=\pm 2$ transition of the $2\nu_6$ vibrational level of HCCCN (1000 cm^{-1} in energy). No lines of HCCCN $\nu_6 = 1, 2$ are detected in our data from the J=9-8 up to J=16-15 rotational transitions of these levels (see also Cernicharo et al. (2000)). The only vibrational level detected so far for HCCCN is the $\nu_7=1$ at $\simeq 100\text{ cm}^{-1}$. Hence, we are confident that this feature is unknown previous to its assignment to HMgNC. The J=12-11 transition of HMgNC at 131534.4(5) MHz is slightly contaminated in its red part by a narrow, half power linewidth $\simeq 3\text{ MHz}$, and weak feature of HCN in its $\nu_1 + 3\nu_2 + \nu_3$ vibrational mode (Cernicharo et al. 2011). The CCS line in the high frequency part of the line profile is separated by 17 MHz from the J=12-11 transition of HMgNC and is not affecting the line profile. Consequently, the HMgNC line is clearly detected with a signal to noise ratio (SNR) of > 6 . Finally, the J=13-12 transition is predicted at 142491.8(7) MHz. It is partially blended with the 11_{11} - 10_{10} line of CCS at 142501.694(6) MHz. At this frequency the full linewidth of the IRC+10216 features is 13.8 MHz. As the HMgNC and CCS lines are separated by 10 MHz 70% of the HMgNC line profile is free of contamination by CCS (note that this spectrum has a sensitivity of 0.6 mK). The U shaped profile of the lines arising in the shell where radicals have been found is clearly visible in all the observed lines. The rotational constants of HMgNC can be slightly improved by fitting the space frequencies together with the laboratory ones. We obtain $B_0=5481.4336(4)\text{ MHz}$ and $D_0=2.94(5)\text{ KHz}$. Predictions for lines with $E_{\text{upper}} < 100\text{ K}$ are given in Table 1.

From the data provided in Figure 2 we obtain for HMgNC $T_{\text{rot}}=21\pm 6\text{ K}$ and $N=(6\pm 2)\times 10^{11}\text{ cm}^{-2}$. Using all the lines of MgNC and MgCN published in previous papers (Guélin et al. 1986; Guélin, Lucas & Cernicharo 1993; Ziurys et al. 1995) we derive for MgNC $T_{\text{rot}}=18.6\pm 1\text{ K}$ and $N=(13\pm 3)\times 10^{12}\text{ cm}^{-2}$. For MgCN we obtain $T_{\text{rot}}=13\pm 3\text{ K}$ and $N=(7.4\pm 2)\times 10^{11}\text{ cm}^{-2}$. The abundance ratio between these species is $N(\text{MgNC})/N(\text{HMgNC})\simeq 20$, $N(\text{HMgNC})/N(\text{MgCN})\simeq 0.8$, and $N(\text{MgNC})/N(\text{MgCN})\simeq 15$.

4. Chemical Modelling and Discussion

The line profiles of HMgNC observed in IRC +10216 have a U shape which indicate that this molecule is formed in the outer shells, as the related radical MgNC (Guélin, Lucas & Cernicharo 1993). The chemistry of HMgNC is highly uncertain –to our knowledge it has not been considered in the past– although it is reasonable to think on the three Mg-bearing molecules detected in IRC +10216 (MgNC, MgCN, and HMgNC) sharing a common origin in the cold

outer envelope. The formation of MgNC in circumstellar sources has been broadly discussed by Petrie (1996) and Dunbar & Petrie (2002), who favour a gas phase formation route driven by the radiative association of Mg^+ and cyanopolyynes



followed by the dissociative recombination of the cation complex. We have implemented the above chemical scheme for Mg in a chemical model of IRC +10216 similar to that by Agúndez et al. (2008). The rate constants for reaction (1) with $n = 3, 5, 7,$ and 9 have been taken from the calculations by Dunbar & Petrie (2002). The analogous reaction with HCN is too slow compared with those involving cyanopolyynes (Petrie 1996). The dissociative recombination of the different cation complexes $\text{Mg}(\text{HC}_{2n+1}\text{N})^+$ with free electrons may ultimately lead to Mg-containing cyanides. However, the branching ratios are unknown and are difficult to predict just based on the exothermicity of the reactions. If this mechanism indeed governs the formation of Mg-bearing molecules in IRC +10216 we should expect the main channel to yield MgNC, based on the relative observed abundances of MgNC, MgCN, and HMgNC. This latter species has a closed shell electronic structure and is thus expected to be less reactive than the two other radicals. We have therefore restricted the loss processes of HMgNC to just photodissociation by interstellar ultraviolet photons, while for MgNC and MgCN we have also considered reactions with H atoms and electrons. The absolute abundances of Mg-bearing molecules scale with the elemental abundance of magnesium in the gas phase, which unfortunately was not constrained by the observations of gas phase atoms in IRC +10216 carried out by Mauron & Huggins (2010).

With this simple chemical scheme we find that in order to reproduce the relative and absolute column densities of the three Mg-bearing molecules observed in IRC +10216, we need a gas phase Mg abundance of 2×10^{-7} relative to H (i.e. depleted by a factor of ~ 200 with respect to the solar abundance) and branching ratios in the dissociative recombination of $\text{Mg}(\text{HC}_{2n+1}\text{N})^+$ ions, which for MgCN and HMgNC are 5 and 1%, respectively, of that of MgNC. In Figure 3 we show the calculated abundances of Mg-bearing species, which are in good qualitative agreement with those obtained by Millar (2008) on MgNC, except for some quantitative differences which are likely to arise from differences in the adopted chemical network. Similarly to Millar (2008), we find that the reactions of radiative association between Mg^+ and cyanopolyynes larger than HC_3N dominate the synthesis of Mg-bearing molecules, due to their higher rate constants. The predicted abundance ratios for MgNC, HMgNC and MgCN are in good agreement with the observations. The putative common chemical origin of MgNC, MgCN, and HMgNC in IRC +10216 may be proven by mapping their emission distribution, which, except for some possible differences in the rotational

excitation and chemical loss processes, should peak at similar angular distances. Investigation on the dissociative recombination of $\text{Mg}(\text{HC}_{2n+1}\text{N})^+$ ions, particularly on the product channels and branching ratios, would also allow to shed light on the chemical synthesis of Mg-bearing molecules, and possibly of other metal-bearing cyanides and isocyanides which have been also detected in IRC +10216. Future observations with ALMA of metal (Mg, Ca, Fe)-bearing radicals and their corresponding hydrogenated closed shell molecules could provide important information on where the different species are formed in the circumstellar envelope and, hence, on their formation mechanism.

The Spanish authors thank the Spanish MICINN for funding support through grants CTQ2010-19008, CSD2009-00038, AYA2009-07304, AYA2012-32032, and Junta de Castilla y León (grant VA070A08).

REFERENCES

- Agúndez, M., Fonfría, J. P., Cernicharo, J., et al. 2008, *A&A*, 479, 493
- Alonso, J. L., Pérez, C., Sanz, M. E., et al., 2009, *Phys. Chem. Chem. Phys.*, 11, 617
- Cabezas, C., Mata, S., Daly, A. M. et al., 2012, *J. Mol. Spectrosc.*, 278, 31
- Cernicharo, J., 1985, Internal IRAM report (Granada: IRAM)
- Cernicharo, J., Kahane, C., Gómez-González, J., & Guélin, M., 1986a, *A&A*, 164, L1
- Cernicharo, J., Kahane, C., Gómez-González, J., & Guélin, M., 1986b, *A&A*, 167, L5
- Cernicharo, J., Guélin, M., 1987, *A&A*, 183, L10
- Cernicharo, J., Guélin, M., Walmsley, 1987a, *A&A*, 172, L5
- Cernicharo, J., Guélin, M., Menten, K.M., Walmsley, 1987b, *A&A*, 181, L1
- Cernicharo, J., Guélin, M., 1996, *A&A*, 309, L27
- Cernicharo, J., Guélin, M., Kahane, C., et al., 2000, *A.&A. SS*, 142, 181
- Cernicharo, J., Agúndez, M., Kahane, C., et al., 2011, *A&A*, 529, L3
- Cernicharo, J., 2012, in *ECLA-2011: Proceedings of the European Conference on Laboratory Astrophysics*, EAS Publications Series, vol 58, 2012, Editors: C. Stehl, C. Joblin, and L. d’Hendecourt (Cambridge: Cambridge Univ. Press), 251

- Dunbar, R. C. & Petrie, S. 2002, *ApJ*, 564, 792
- Gronowski, M., Kolos, R., 2013, *J. Phys. Chem. A*, 117, 4455
- Guélin, M., Gómez-González, J., Cernicharo, J., Kahane, C., 1986, *A&A*, 157, L17
- Guélin, M., Cernicharo, J., Kahane, C., Gómez-González, J., & Walmsley, C.M., 1987, *A&A*, 175, L5
- Guélin, M., Lucas, R., Cernicharo, J., 1993, *A&A*, 280, L19
- Guélin, M., Cernicharo, J., Travers, M.J., et al., 1997, *A&A*, 317, L1
- Guélin, M., Muller, S. Cernicharo, J., et al., 2000, *A&A*, 363, L9
- Guélin, M., Muller, S. Cernicharo, J., et al., 2004, *A&A*, 426, L49
- Highberger, J.L., Thomson, K.J., Young, P.A., et al., 2003, *ApJ*, 593, 393
- Kaminski, T., Gottlieb, C.A., Menten, K.M., et al., 2013, *A&A*, 551, A113.
- Kawaguchi, K., Kagi, E., Hirano, T., et al., 1993, *ApJ*, 406, L39
- Mauron, N., Huggins, P.J., 2010, *A&A*, 513, A31
- Millar, T. J. 2008, *Ap&SS*, 313, 223
- Pardo, J. R., Cernicharo, J., Serabyn, E. 2001, *IEEE Trans. Antennas and Propagation*, 49/12, 1683
- Petrie, S. 1996, *MNRAS*, 282, 807
- Pulliam, R.L., Savage, C., Agúndez, M., et al., 2010, *ApJ*, 725, L181
- Sanz, M.E., McCarthy M.C., Thaddeus, P., 2002, *ApJ*, 577, L71
- Tsuji, T., 1973, *A&A*, 23, 411
- Turner, B.E., Steimle, T.C., & Meerts, L., 1994, *ApJ*, 426, L97
- Walker, K. A. & Gerry, M. C. L., 1998, *J. Mol. Spectrosc.*, 189, 40
- Zack, L.N., Halfen, D.T. & Ziurys, L.M., 2011, *ApJ*, 733, L36
- Ziurys, L.M., Apponi, A.J., Guélin, M., & Cernicharo, J., 1995, *ApJ*, 445, L47
- Ziurys, L.M., Savage, C., Highberger, J.L., et al., 2002, *ApJ*, 564, L45

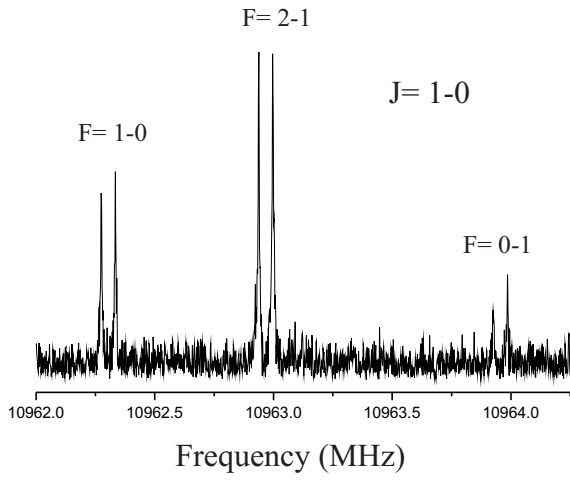


Fig. 1.— $J=1-0$ rotational transition of HMgNC, observed in this work near to 11 GHz. The nuclear quadrupole coupling hyperfine structure is clearly resolved. This spectrum represents one scan at steps of 0.3 MHz with 600 averages phase-coherently coadded in each point.

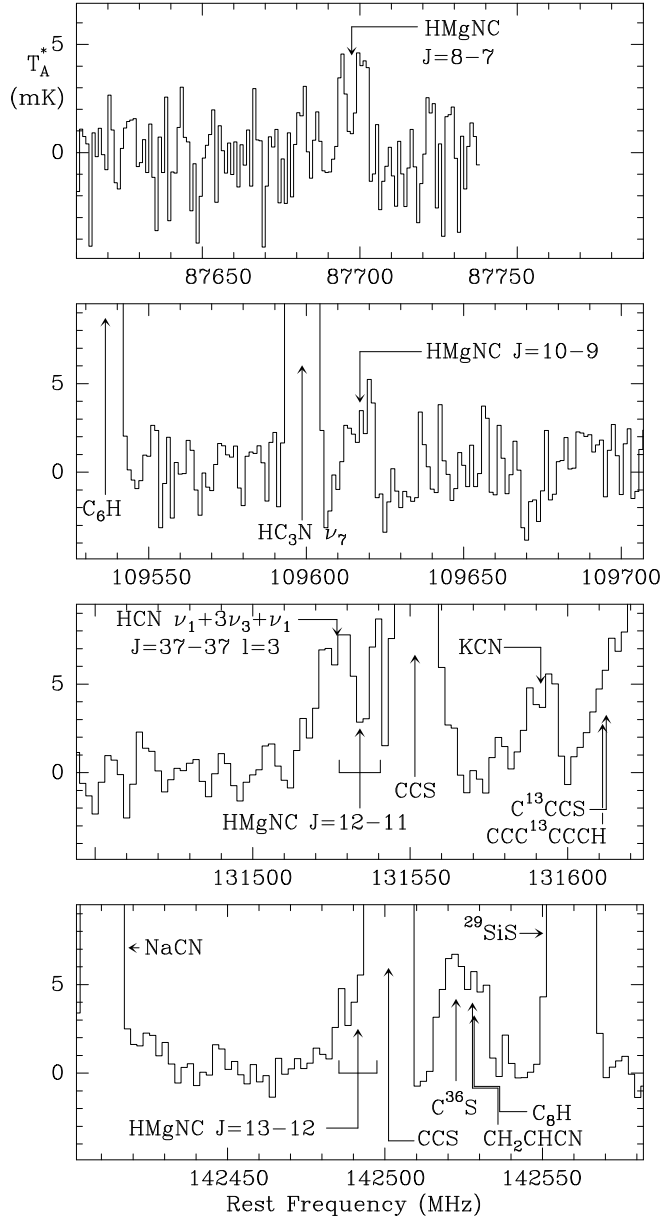


Fig. 2.— Observed transitions of HMgNC towards IRC+10216. The horizontal scale corresponds to the rest frequency assuming a V_{LSR} of -26.5 km s^{-1} . The intensity scale is antenna temperature in mK corrected for atmospheric attenuation and telescopes losses. The $J=9-8$ line is fully blended with a line of H_2C_4 and it is not shown. The $J=12-11$ is partially blended with a narrow and weak transition of HCN coming from the dust formation zone (Cernicharo et al. 2011). The $J=13-12$ line is also partially blended with a line of CCS but 80% of the frequency coverage of the HMgNC line is free of contamination and appears clearly detected. This spectrum has a sensitivity of 0.6 mK (1σ). The whole frequency coverage of the $J=12-11$ and $J=13-12$ transitions is indicated.

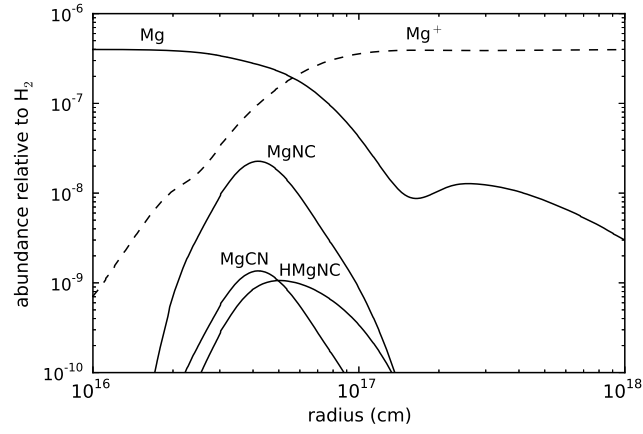


Fig. 3.— Calculated abundances of Mg-bearing species in IRC +10216 as a function of the radial distance.